REPORT

CELL SIGNALING

A macrophage relay for long-distance signaling during postembryonic tissue remodeling

Dae Seok Eom and David M. Parichy*†

Macrophages have diverse functions in immunity as well as in development and homeostasis. We identified a function for these cells in long-distance communication during postembryonic tissue remodeling. Ablation of macrophages in zebrafish prevented melanophores from coalescing into adult pigment stripes. Melanophore organization depends on signals provided by cells of the yellow xanthophore lineage via airinemes, long filamentous projections with vesicles at their tips. We show that airineme extension from originating cells, as well as vesicle deposition on target cells, depend on interactions with macrophages. These findings identify a role for macrophages in relaying long-range signals between nonimmune cells. This signaling modality may function in the remodeling and homeostasis of other tissues during normal development and disease.

Macrophages are phagocytic cells with essential roles in immunity, including recognition and disposal of infectious microbes, dying cells, and debris. Yet nonimmune activities have also been identified. Macrophages are now known to function during development and homeostasis, including blood vessel and mammary duct morphogenesis, pancreatic cell specification, hematopoietic stem cell maintenance, and lipid metabolism (*1*–*4*). To investigate potential roles for macrophages in postembryonic tissue remodeling, we examined the larval-to-adult transformation of zebrafish, a period of morphogenesis, patterning, and growth with similarities to human fetal and neonatal development (*5*, *6*).

We depleted macrophage populations by expressing bacterial nitroreductase (NTR) in these cells. NTR kills cells by converting metronidazole (Mtz) to toxic metabolites (*7*, *8*) (fig. S1). Fish treated with Mtz between mid-larval and juvenile stages had a severe defect in the adult pattern of neural crest–derived pigment cells. Untreated juvenile zebrafish exhibit dark stripes of black melanophores dorsal and ventral to a light "interstripe" of yellow-orange xanthophores and iridescent iridophores. Yet macrophage-depleted fish retained numerous melanophores in the interstripe (Fig. 1A and fig. S2). This pattern resembled a phenotype that results from a defect in long-distance communication between melanophores and xanthophore precursors (*9*).

During stripe development, progenitors of adult melanophores migrate to the skin and begin to differentiate widely over the flank (*10*). At this stage, precursors to adult xanthophores are already located in the prospective interstripe, where they differentiate as xanthophores, and also in prospective stripes, where they remain as unpigmented xanthoblasts (*6*) (Fig. 2A). Interactions between melanophores and cells of the xanthophore lineage are required for pattern formation and maintenance (*11*–*14*); for example, xanthophores repel melanophores at short range (*15*, *16*). By contrast, xanthoblasts extend thin projections, "airinemes," that contact dispersed melanophores and melanoblasts (*9*). Airinemes arise from surface blebs, can reach up to several cell diameters (>150 μm), and have large (~1 μm) membrane-bound vesicles at their tips that harbor the Notch pathway ligand DeltaC and potentially other factors. When xanthoblasts are ablated, or when airineme production or Delta-Notch signaling are inhibited, melanophores fail to organize and many persist in the interstripe (*9*). Given the similarity of this phenotype to that of macrophage depletion, we speculated that macrophages contribute to airineme-dependent signaling.

To test for correspondence in macrophage and airineme behaviors, we used time-lapse imaging. The haphazard wanderings of macrophages, revealed by an *mpeg1* reporter (*8*), were qualitatively similar to the haphazard paths taken by airineme vesicles, as revealed by a membrane-targeted *aox5* reporter (*6*, *9*) (Fig. 2B and fig. S3). To see whether macrophages and airinemes interact, we examined both reporters simultaneously (fig. S1D). Of 178 airinemes, 168 (94%) were associated with macrophages, although limits on temporal resolution and detection in deeper tissues may have prevented all macrophages from being seen. Airinemes extended in association with macrophages traversing xanthoblasts and, while airinemes were extending, their vesicles remained associated with macrophages for up to 189 μm (Fig. 2C, fig. S4A, and movies S1 to S4). Interactions occurred between macrophages and airineme vesicles rather than filaments. In 3 of 168 instances, portions of macrophage-associated vesicles detached from trailing filaments and airineme extension continued in association with a second macrophage (fig. S4B and movie S5).

To better understand macrophage-airineme relationships, we used an *mfap4* membrane-targeted reporter of macrophages (*17*) (fig. S1B), which revealed intact airineme vesicles engulfed by macrophages, with filaments trailing back to source xanthoblasts (Fig. 3A and movie S6). These observations suggested the hypothesis that macrophages drag airineme vesicles and filaments from surface blebs of xanthoblasts, much as optical tweezers can pull tethered surface blebs from cells in culture (*18*). If so, we predicted that depleting the macrophage population should reduce the incidence of airineme extension. In support of this idea, Mtz depletion of NTR^+ macrophages markedly reduced airineme incidence (Fig. 3, B and D, fig. S5, and movie S7). As a second paradigm, we used cell transplantation to construct fish with xanthoblasts but not macrophages. Mutants for *colony stimulating*

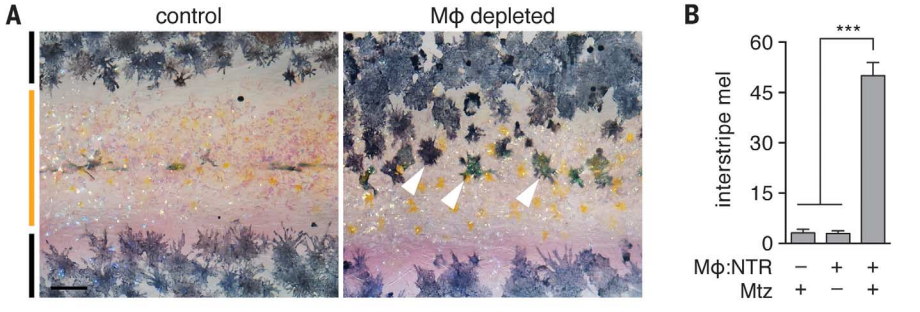

Fig. 1. Macrophage depletion results in melanophore pattern defect. (**A**) In controls, melanophores in stripes (denoted by black bars at far left) border the interstripe (orange bar). Macrophage (Mϕ) depletion results in ectopic melanophores (arrowheads). Scale bar, 100 μm. (**B**) Macrophage-depleted fish (NTR^+, Mtz^+) had many more melanophores in the interstripe than did controls ($F_{2,17}$ = 95.7, P < 0.0001; N = 20 larvae total), although total melanophore numbers did not differ ($F_{2,17}$ = 1.0, P = 0.4); data are means ± SE. ***Both comparisons P < 0.0001; stage 13 standardized standard length (SSL) (*5*).

Department of Biology, University of Washington, Seattle, WA 98195, USA.
*Present address: Department of Biology, University of Virginia, Charlottesville, VA 22904, USA. †**Corresponding author. Email: dparichy@virginia.edu**

factor-1 receptor a (*csf1ra*) are deficient for macrophages but also for xanthophores and xanthoblasts (*19*, *20*). We therefore transplanted cells from wild-type embryos carrying lineage reporters into *csf1ra* mutant embryos, and reared chimeras that developed xanthoblasts but not macrophages (*aox5*$^+$, *mpeg1*$^-$). These larvae exhibited far fewer airinemes than macrophage-intact wild-type hosts (Fig. 3C, fig. S6A, and movie S8). We observed similar macrophage dependencies even in a background with particularly exuberant airinemes (fig. S6, B and C, and movies S9 and S10) (*9*). In all paradigms, the few airinemes extended were associated with residual macrophages (movie S11). Thus, macrophages are essential for airineme extension.

Macrophages provide a variety of signals to target cells (*2*–*4*, *21*) but did not influence the competence of xanthoblasts to initiate airineme formation; surface blebs from which airinemes arise (*9*) were similarly abundant in control and macrophage-depleted backgrounds (fig. S7A). Likewise, neither onset nor cessation of peak airineme activity were associated with specific changes in macrophage abundance (fig. S7B).

We therefore asked how macrophages recognize airineme-initiating blebs when they are present. DeltaC localizes to these blebs (*9*), yet airinemes developed normally in *delta c* mutants, suggesting roles for other factors (fig. S7C). On apoptotic cells, the phospholipid phosphatidylserine (PS) occurs in the outer leaflet of the plasma membrane, where it serves as an "eat me" signal for macrophages (*21*, *22*). Accordingly, we hypothesized that xanthoblast blebs present PS to macrophages. To detect PS, we delivered a secreted form of PS-binding Annexin V, SecA5-mCherry, into the tissue environment of xanthoblasts by expressing it in nearby melanophores or iridophores (*10*, *23*–*25*). We found strong secA5 labeling of airineme-initiating blebs on xanthoblasts and an absence of labeling on xanthophores, which formed neither blebs nor airinemes (Fig. 3E and fig. S8). If PS is required for macrophage-bleb recognition, we predicted that PS-secA5 interaction should block airineme extension. Indeed,

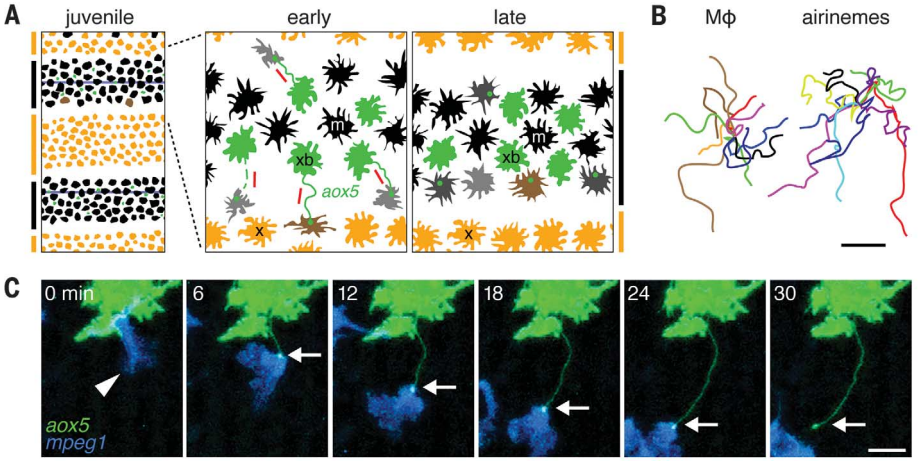

Fig. 2. Correspondence of macrophage movements with xanthoblast-derived airineme projections. (**A**) Consolidation of melanophore stripes depends on interactions with cells of the xanthophore lineage. Schematic of the juvenile pattern showing a region corresponding to Fig. 1A (outlined in blue) with enlargements of a stripe region illustrating prior events early and late in stripe formation. Xanthoblasts (green; xb marked by *aox5*) among melanophores (m) extend airinemes (red bars) that contact differentiating melanophores (gray) or embryonic melanophores persisting in the interstripe (brown); airineme vesicles can persist on melanophores for several hours, even after filaments have fragmented. Several days later, airinemes are no longer produced and melanophores have consolidated into definitive stripes. Xanthophores (orange; x) occur in the interstripe. (**B**) Similar wanderings of macrophages and airineme vesicles (colors represent paths taken by individual macrophages or vesicles; starting positions at center). (**C**) A macrophage (blue, arrowhead) that has traversed a single xanthoblast (green; 0 min) associated with an airineme vesicle (arrow) and trailing filament (6 to 24 min); airineme extension ceased upon macrophage-vesicle dissociation (24 to 30 min). Scale bars, 40 μm (B), 20 μm (C).

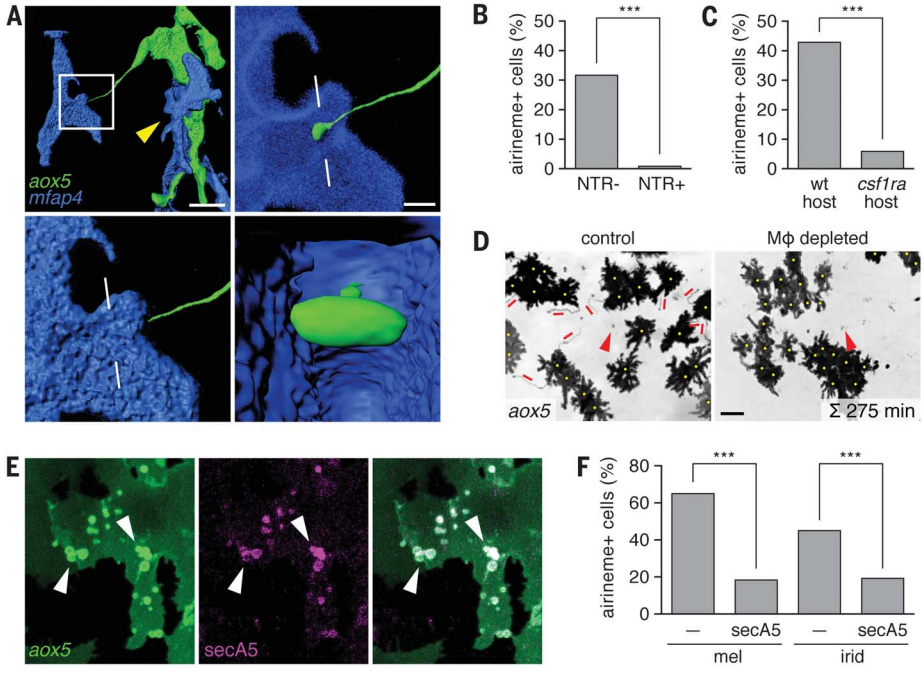

Fig. 3. Macrophage requirements for airineme extension. (**A**) Xanthoblast (green) and macrophages (blue) illustrating close association (arrowhead) and engulfment of airineme vesicle with filament. White boxed region shown with and without surface rendering of macrophage in lower right and upper left; hatch marks, cut plane inside macrophage at lower right. (**B**) Xanthoblasts of macrophage-depleted fish (NTR$^+$) were less likely than controls (NTR$^-$) to extend airinemes (χ^2 = 52.0, df = 1, P < 0.0001, N = 284 cells, 14 larvae). (**C**) Xanthoblasts in macrophage-deficient *csf1ra* mutant hosts similarly had fewer airinemes than wild-type hosts (χ^2 = 23.8, df = 1, P < 0.0001, N = 198 cells, 9 larvae). (**D**) Merged time-lapse frames illustrate airinemes (red dashes) in control (NTR$^-$) but not macrophage-depleted (NTR$^+$) trunks. Yellow dots, approximate cell centroids; arrowheads, autofluorescence in cells not carrying *aox5* reporter. (**E**) PS localization at airineme-originating blebs (arrowheads) of a single xanthoblast detected by secA5. (**F**) Airineme extension was repressed in the vicinity of secA5-expressing melanophores (mel; χ^2 = 146.4, df = 1, P < 0.0001, N = 626 cells, 15 larvae) and iridophores (irid; χ^2 = 16.7, df = 1, P < 0.0001, N = 215 cells, 8 larvae), although macrophage motility (μm/min) did not differ between secA5$^-$ and secA5$^+$ regions (t_{54} = 0.8, P = 0.4; N = 56 cells, 6 larvae). ***P < 0.0001. Scale bars, 10 μm [(A), upper left], 2 μm [(A), upper right], 50 μm (D).

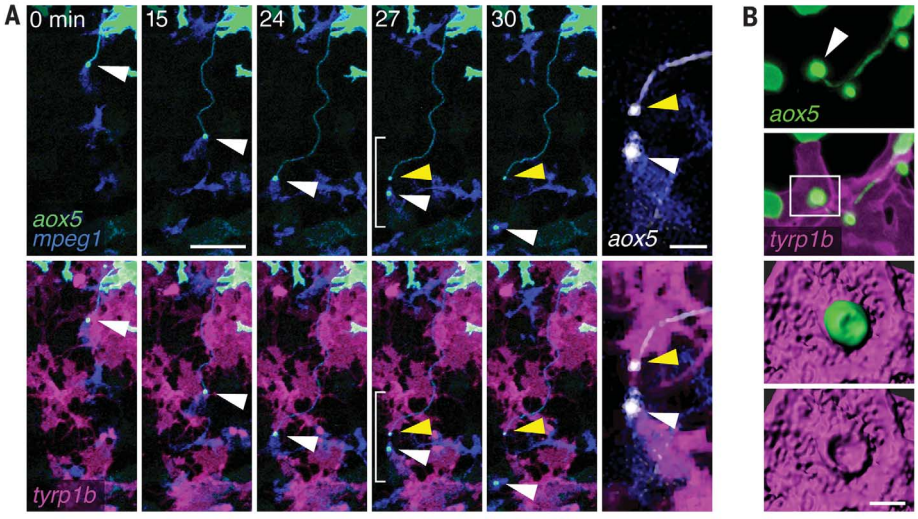

Fig. 4. Macrophages relay airineme vesicles to melanophores. (**A**) Airineme vesicle (green) associated with a macrophage (blue; two-color merge, upper panels) and melanophores (magenta; three-color merge, lower panels). The airineme extended as the macrophage migrated (0 to 24 min, white arrowhead), but a portion of the vesicle and its filament then stabilized on the melanophore (27 min, yellow arrowhead) as the macrophage continued on with some vesicular material (30 min). The rightmost panels show expanded images of the bracketed region at 27 min. (**B**) Airineme vesicle associated with melanophore membrane. The boxed region is surface-rendered in the lower panels. Scale bars: 50 μm [(A), main panels]; 10 μm [(A), rightmost panels]; 2 μm [(B), lower panels].

airinemes were produced less often in the vicinity of secA5^{+} cells than secA5^{-} cells (Fig. 3F). These observations suggest that a macrophage-PS recognition system has been co-opted for airineme extension and long-distance communication.

Our observations indicate that macrophages may relay signals, associated with airineme vesicles, from xanthoblasts to melanophores. We therefore sought to verify that macrophage-borne airineme vesicles can be deposited on melanophores, and to test whether macrophages remain with vesicles after delivery. In fish transgenic for a membrane-targeted *tyrp1b* reporter (*6*) of melanophores, macrophage-borne airineme vesicles were deposited frequently on melanophores, without indications of membrane fusion or internalization; macrophages did not cease their movements after vesicle "hand-off" and instead continued to wander (Fig. 4 and movies S12 and S13). Because patterning can depend on attenuation of signals, we also asked whether macrophages might dispose of previously extended airineme vesicles. We observed macrophages phagocytosing vesicles that had stabilized on melanophores, as well as vesicles that had been extended without stabilizing (movies S14 and S15). Thus, macrophages not only mediate signaling to melanophores, they also may regulate the duration and specificity of signaling.

Communication at a distance is fundamentally important to patterning, yet its mechanisms remain incompletely understood. Considerable attention has been given to signaling via long actin-based filopodia, or "cytonemes" (*26*, *27*), yet additional classes of cellular projections have been identified, the properties of which are only beginning to be explored (*28*, *29*). Our analyses show that macrophages are key players in long-range, airineme-dependent communication between xanthoblasts and melanophores. Indeed, macrophage wanderings may allow for diffusion-like dissemination, envisaged by mathematical models (*13*, *30*), despite the large size of airineme vesicles and the long distances involved. Our findings add to the increasingly diverse recognized functions of macrophages, defined classically for their phagocytic capabilities. It remains to be determined whether macrophages passively carry signals, actively process them, or assist in discriminating among target cells (*9*). Identifying additional features of macrophage-airineme interactions in this context, and potentially other contexts, will shed light on the evolution and generality of this system and may also suggest novel approaches for delivery of therapeutic agents.

REFERENCES AND NOTES

1. A. I. Tauber, *Nat. Rev. Mol. Cell Biol.* **4**, 897–901 (2003).
2. J. A. Stefater 3rd, S. Ren, R. A. Lang, J. S. Duffield, *Trends Mol. Med.* **17**, 743–752 (2011).
3. T. A. Wynn, A. Chawla, J. W. Pollard, *Nature* **496**, 445–455 (2013).
4. F. Ginhoux, S. Jung, *Nat. Rev. Immunol.* **14**, 392–404 (2014).
5. D. M. Parichy, M. R. Elizondo, M. G. Mills, T. N. Gordon, R. E. Engeszer, *Dev. Dyn.* **238**, 2975–3015 (2009).
6. S. K. McMenamin *et al.*, *Science* **345**, 1358–1361 (2014).
7. S. Curado, D. Y. Stainier, R. M. Anderson, *Nat. Protoc.* **3**, 948–954 (2008).
8. T. A. Petrie, N. S. Strand, C. T. Yang, J. S. Rabinowitz, R. T. Moon, *Development* **141**, 2581–2591 (2014).
9. D. S. Eom, E. J. Bain, L. B. Patterson, M. E. Grout, D. M. Parichy, *eLife* **4**, e12401 (2015).
10. E. H. Budi, L. B. Patterson, D. M. Parichy, *PLOS Genet.* **7**, e1002044 (2011).
11. D. M. Parichy, J. M. Turner, *Development* **130**, 817–833 (2003).
12. H. Hamada *et al.*, *Development* **141**, 318–324 (2014).
13. M. Watanabe, S. Kondo, *Trends Genet.* **31**, 88–96 (2015).
14. U. Irion, A. P. Singh, C. Nüsslein-Volhard, *Curr. Top. Dev. Biol.* **117**, 141–169 (2016).
15. A. Nakamasu, G. Takahashi, A. Kanbe, S. Kondo, *Proc. Natl. Acad. Sci. U.S.A.* **106**, 8429–8434 (2009).
16. M. Inaba, H. Yamanaka, S. Kondo, *Science* **335**, 677 (2012).
17. E. M. Walton, M. R. Cronan, R. W. Beerman, D. M. Tobin, *PLOS ONE* **10**, e0138949 (2015).
18. J. Dai, M. P. Sheetz, *Biophys. J.* **77**, 3363–3370 (1999).
19. D. M. Parichy, D. G. Ransom, B. Paw, L. I. Zon, S. L. Johnson, *Development* **127**, 3031–3044 (2000).
20. P. Herbomel, B. Thisse, C. Thisse, *Dev. Biol.* **238**, 274–288 (2001).
21. J. Savill, I. Dransfield, C. Gregory, C. Haslett, *Nat. Rev. Immunol.* **2**, 965–975 (2002).
22. A. Hochreiter-Hufford, K. S. Ravichandran, *Cold Spring Harb. Perspect. Biol.* **5**, a008748 (2013).
23. S. Krahling, M. K. Callahan, P. Williamson, R. A. Schlegel, *Cell Death Differ.* **6**, 183–189 (1999).
24. T. J. van Ham, J. Mapes, D. Kokel, R. T. Peterson, *FASEB J.* **24**, 4336–4342 (2010).
25. L. B. Patterson, D. M. Parichy, *PLOS Genet.* **9**, e1003561 (2013).
26. C. L. Fairchild, M. Barna, *Curr. Opin. Genet. Dev.* **27**, 67–73 (2014).
27. T. B. Kornberg, S. Roy, *Development* **141**, 729–736 (2014).
28. M. C. McKinney, D. A. Stark, J. Teddy, P. M. Kulesa, *Dev. Dyn.* **240**, 1391–1401 (2011).
29. M. Inaba, M. Buszczak, Y. M. Yamashita, *Nature* **523**, 329–332 (2015).
30. H. Meinhardt, A. Gierer, *Bioessays* **22**, 753–760 (2000).

ACKNOWLEDGMENTS

We thank A. Aman, E. Bain, S. Larson, T. Larson, M. Roh-Johnson, and J. Wallingford for discussions, critical reading of the manuscript, or both. Supported by NIH grant R01 GM096906 (D.M.P.). Author contributions: D.S.E. performed experiments; D.S.E. and D.M.P. designed the experiments, analyzed data, and wrote the manuscript.

SUPPLEMENTARY MATERIALS

www.sciencemag.org/content/355/6331/1317/suppl/DC1
Materials and Methods
Figs. S1 to S8
Movies S1 to S16
References (*31*–*33*)

25 October 2016; accepted 3 February 2017
Published online 16 February 2017
10.1126/science.aal2745

Science
AAAS

A macrophage relay for long-distance signaling during postembryonic tissue remodeling

Dae Seok Eom and David M. Parichy (February 16, 2017)
Science **355** (6331), 1317-1320. [doi: 10.1126/science.aal2745]
originally published online February 16, 2017

Editor's Summary

Cell projections set up pigment pattern

Macrophages eliminate dead or dying cells and identify and destroy invading microbes. However, they also exhibit nonimmune functions in development and homeostasis. Eom and Parichy show that macrophages are essential for postembryonic remodeling during adult pigment stripe formation in zebrafish (see the Perspective by Guilliams). Pigment cells relay signal-containing vesicles via cellular projections from one class of cell to another. Without macrophages, this signal relay fails, and adult stripes are disorganized.

Science, this issue p. 1317; see also p. 1258

Science (print ISSN 0036-8075; online ISSN 1095-9203) is published weekly, except the last week in December, by the American Association for the Advancement of Science, 1200 New York Avenue NW, Washington, DC 20005.

www.sciencemag.org/cgi/content/full/science.aal2745/DC1

Supplementary Materials for

A macrophage relay for long-distance signaling during postembryonic tissue remodeling

Dae Seok Eom and David M. Parichy*

*Corresponding author. Email: dparichy@uw.edu

Published 16 February 2017 on *Science* First Release
DOI: 10.1126/science.aal2745

This PDF file includes:

Other supplementary material for this manuscript includes the following:

Movies S1 to S16

Materials and Methods

Staging, fish rearing and genetic stocks

Staging followed ref. (5) and fish were maintained at 28.5 °C, 16:8 light:dark. Zebrafish were wild-type AB^{wp} or its derivative WT(ABb), as well as: *csf1ra*^{j4e1} [ref. (19)]; *Tg(tg:nVenus-2a-NTR)*$^{wp.rt8}$, *Tg(aox5:PALM-EGFP)*$^{wp.rt22}$, *Tg(tyrp1b:PALM-mCherry)*$^{wp.rt11}$ [ref. (6)]; *Tg(mpeg1:Brainbow)*^{w201} [ref. (31)], which expresses tdTomato in the absence of Cre-mediated recombination, provided by L. Ramakrishnan; *Tg(mfap4:Tomato-CAAX)*^{xt6} provided by D. Tobin [ref. (17)]; and *Tg(mpeg1:NTR-eYFP)*^{w202} from R. Moon [ref. (8)]. Because experiments were analyzed prior to development of secondary sexual characteristics, it was not feasible to identify sexes of individuals prospectively; all stocks used yield approximately balanced sex ratios so experiments are likely to have sampled similar numbers of males and females. All rearing and experiments were conducted with approval of the University of Washington Institutional Animal Care and Use Committee (protocol #4094-01) in accordance with institutional and federal guidelines for the ethical use of animals.

Drug treatments

For macrophage ablation experiments, *Tg(mpeg1:NTR-eYFP)* or non-transgenic sibling controls at 7.5 SSL were treated with 10 mM Mtz overnight (Sigma-Aldrich), and treatment was continued during time-lapse imaging (see below). For long-term macrophage ablation, fish were treated beginning at 6.5 SSL and extending through 13 SSL with 7 mM Mtz administered during dark cycles only, as uninterrupted Mtz treatment curtailed feeding behavior. To generate fish lacking thyroid hormone, thyroid follicles of *Tg(tg:nVenus-2a-nfnB)* fish were ablated at 4 days post-fertilization by treatment with 10 Mm Mtz for 4 h (6).

Time-lapse and still imaging

Pigment cells and macrophages were imaged "*ex vivo*" in their native tissue environment using explanted larval trunks as described [refs. (9, 10)], allowing for longer duration analyses as compared to intact fish imaged similarly. Airineme extension behaviors and frequencies did not differ between *ex vivo* and intact imaging modalities (fig. S3; movie S4). Airineme morphologies also did not depend on the specific fluorophores or targeting motifs (palm-EGFP, EGFP-CAAX, tubulin-mCherry; fig. S3A). Images were acquired at 2–5 min intervals for 18 h using an Evolve (Photometrics) camera mounted on a Zeiss Observer Z1 inverted microscope with CSU-X1 laser spinning disk (Yokogawa) or on a Zeiss LSM 800 laser scanning confocal microscope. Larvae were 7.5 SSL except where indicated. Levels of acquired images were adjusted to visualize dimly fluorescent airinemes, typically resulting in overexposure of cell bodies, which were otherwise distinguishable by position, cell boundaries, and differences in fluorescence intensity in the mosaic background. Super resolution images were acquired with a Zeiss LSM 800 equipped with Airyscan detector and processed using the Isosurface rendering function of Imaris 8.0 (Bitplane).

Neutral red staining

To visualize phagocytic macrophages, fish at 7.5 SSL were incubated in fish water containing 2.5 µg/ml neutral red (Sigma-Aldrich) at 28.5 °C for 3–4 h, rinsed in fresh water then imaged 1–2 h later.

Cell counts and distributions

To assess melanophore numbers and pattern, melanosomes were contracted towards cell centers with epinephrine to facilitate counts and assessment of cell centroids using the Cell Counter plug-in of Image J (NIH). Each cell was assigned to one or twenty bins from dorsal (0.0) to ventral (1.0) and total numbers of melanophores within each bin were averaged across individuals. Positions of interstripe regions were indicated by nearly melanophore-free troughs in melanophore distributions of controls (positions 0.40, 0.45, 0.50) (9).

Cell transplantation

Chimeric fish were generated by transplanting cells at blastula stages (9, 11), from fish transgenic for *mpeg1:tdTomato-CAAX*, *aox5:PALM-EGFP*, or both to wild-type or *csf1ra* mutant hosts, transgenic or not for *tg:nVenus-2a-NTR*.

Annexin V labeling and analysis

The occurrence of PS in xanthoblast blebs was first assessed in vitro using a fluorophore-conjugated Annexin V probe. To examine PS in vivo, we subcloned secA5 from pBH-UAS-secA5-YFP (Addgene plasmid #32359) upstream of mCherry in a Tol2kit Gateway middle entry vector (32) and expressed this construct in melanophores or iridophores [*mitfa* and *pnp4a* promoters, respectively (9)]. Because *mitfa* expression resulted in secA5-mCherry expression in most melanophores, we compared behaviors of cells in time-lapse imaging between *mitfa:secA5*-mCherry injected and uninjected (secA5–) larvae. Given more limited expression of *pnp4a:secA5*-mCherry, it was possible to select comparable secA5+ and secA5– regions prior to imaging for comparison within larvae. Macrophage counts and behaviors were examined in 150 μm^2 regions at the onset of imaging.

Statistical analysis

Analysis were performed with JMP 8.0 (SAS Institute, Cary NC). Frequency data for behaviors or individual cells were assessed by maximum likelihood. Continuous data were assessed by analyses of variance, using *ln*-transformation to correct residuals for normality and homoscedasticity. Post hoc means were compared by Turkey Kramer HSD.

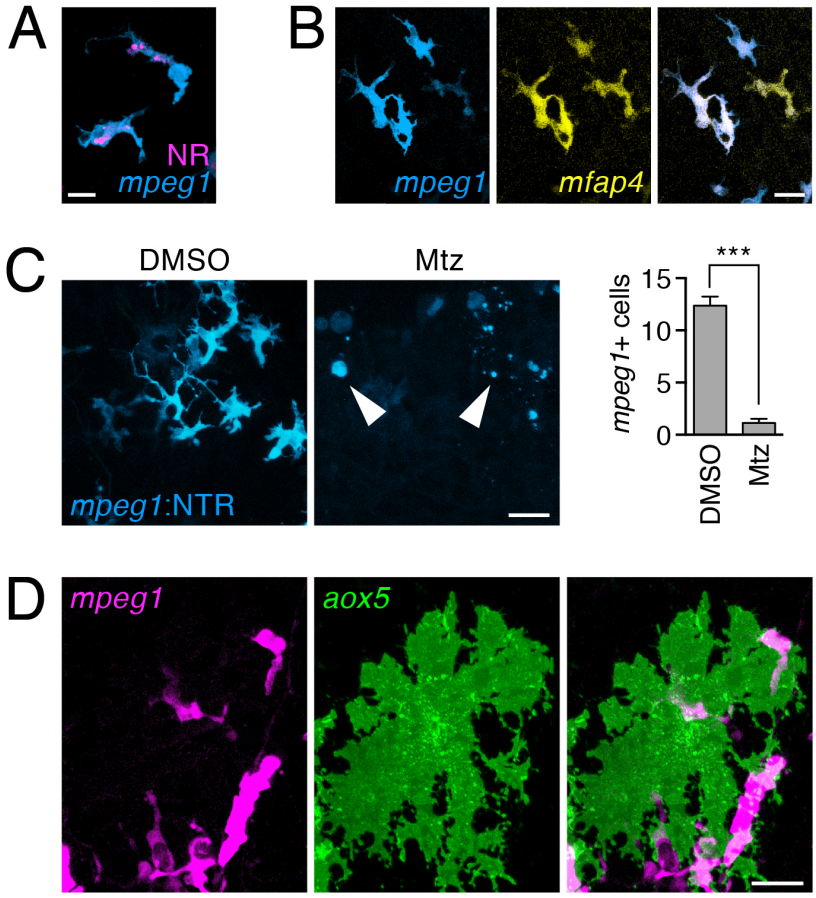

Supplementary figure S1. Macrophage reporters and depletion. (**A**) Coincidence of phagocytosed neutral red (NR, red) and *mpeg1*$^{+}$ macrophage (blue). (**B**) Coexpression of fluorophores driven by *mpeg1* (blue) and *mfap4* (yellow) promoters. (**C**) Mtz treatment kills NTR+ macrophages. Arrowheads, cell debris. Plot shows mean±SE *mpeg1*+ cells observed at start of time-lapse imaging (t_{14}=11.8, P<0.0001). (**D**) Macrophage reporters are not expressed by cells of the xanthophore lineage; shown are several macrophages (*mpeg1*, magenta) and a single xanthoblast (*aox5*, green). See text for details. Scale bars: 10 μm (A); 20 μm (B,D); 20 μm (C).

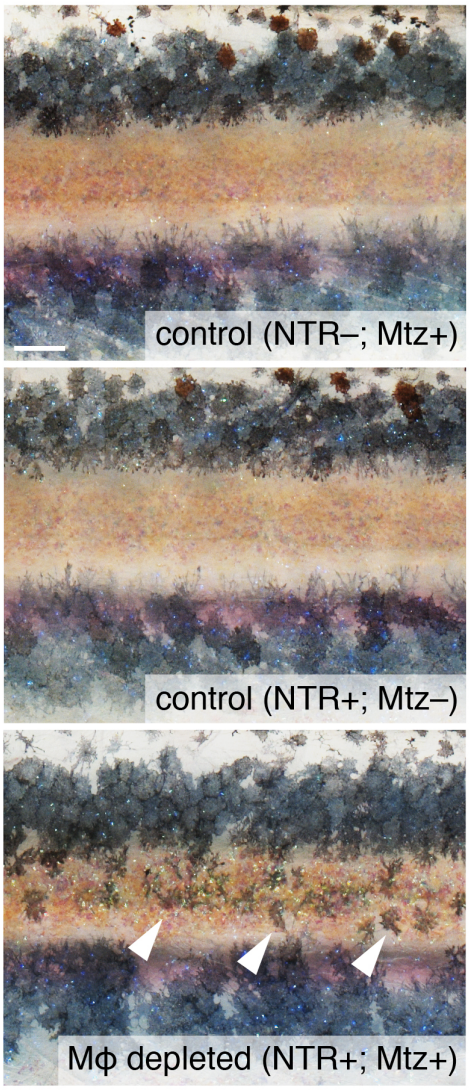

Supplementary figure S2. Macrophage-dependent stripe patterning. Representative juvenile fish (13 SSL) with intact macrophages (upper two panels) or depleted macrophages (lower panel), showing macrophage requirement for melanophore clearance from the interstripe (arrowheads). Scale bar: 100 μm.

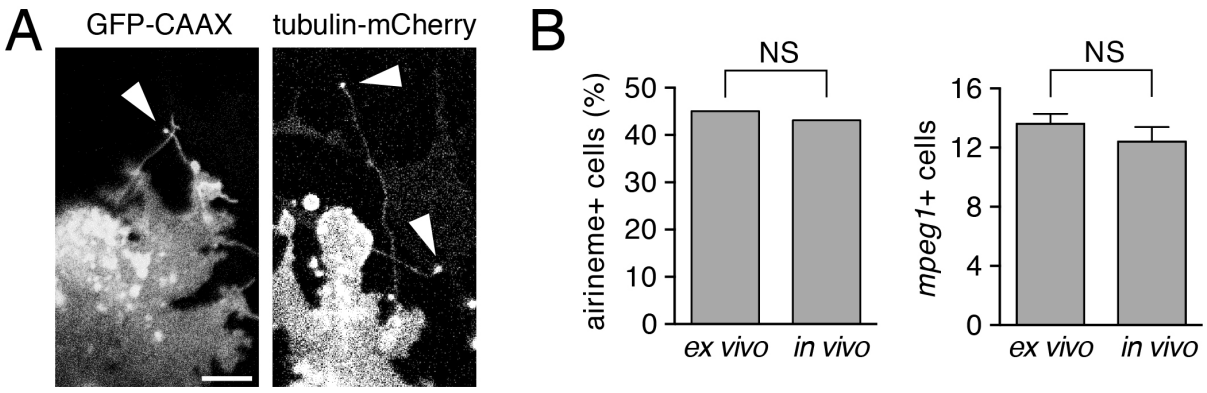

Supplementary figure S3. Xanthoblast airinemes and comparison of cell behaviors observed by time-lapse imaging of trunk explants and intact larvae. (**A**) Airineme behaviors and features are independent of fluorophores used as vesicles and filaments can be observed with membrane-targeted palm-EGFP (main text and other supplementary figures), palm-mCherry (9), EGFP-CAAX (arrowhead, left panel), and reporters not targeted to membranes such as tubulin-mCherry (arrowheads, right panel). (**B**) As seen in other contexts (9, 10, 33), behaviors of cells in explanted trunks (*ex vivo*) recapitulates that of cells in intact larvae (*in vivo*) as observed by time-lapse imaging, with no significant difference between imaging paradigms in either incidence of airineme extension (χ^2=0.1, d.f.=1, *P*=0.8, *N*=156 cells, 11 larvae) or mean±SE numbers of *mpeg1*+ macrophages observed ($F_{1,11}$=0.7, *P*=0.4). Scale bar: 10 μm (A).

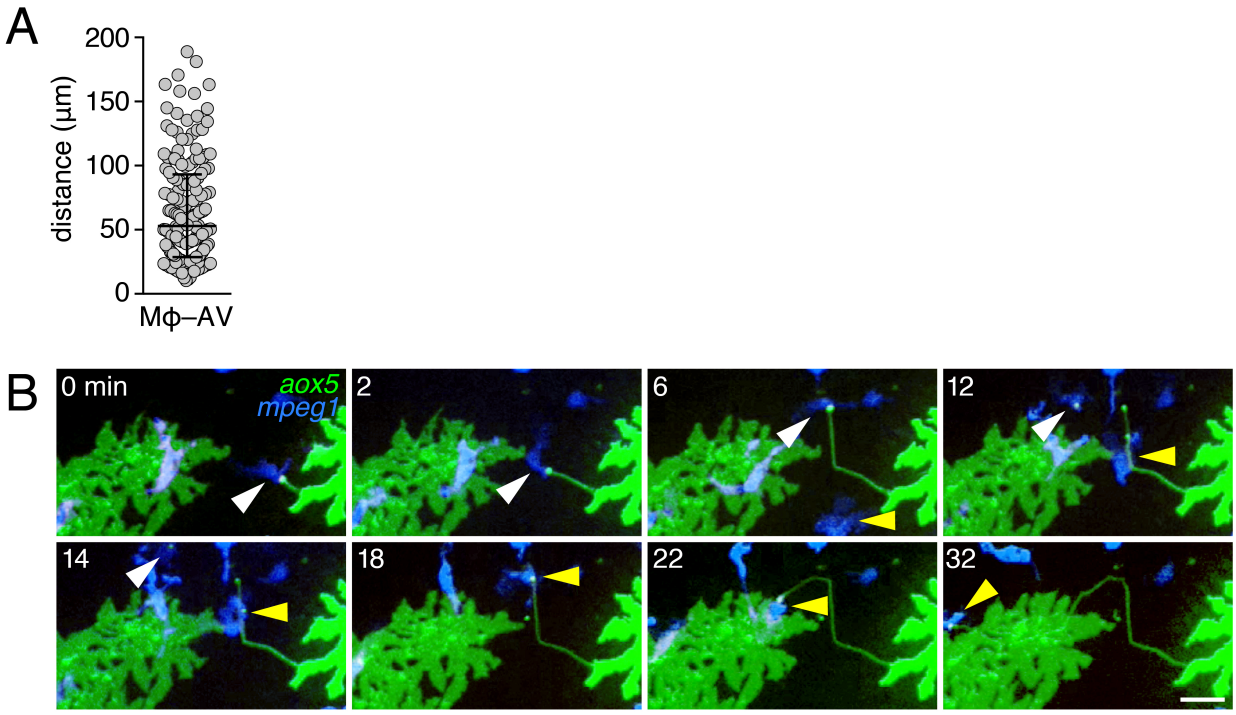

Supplementary figure S4. Airineme extension distances and interactions with multiple macrophages. (**A**) Macrophage-associated airineme vesicles (MΦ–AV) traveled long distances (median ± interquartile range; *N*=168). (**B**) Frames illustrating an initial association between macrophage, airineme vesicle and extending filament (white arrowhead, 0–6 min). This macrophage continued migrating with a portion of airineme vesicle after it dissociated from the trailing filament (12 min). A second macrophage (yellow arrowhead) then associated with vesicle remaining at the airineme tip and airineme extension continued (12–32 min). Scale bar: 20 µm.

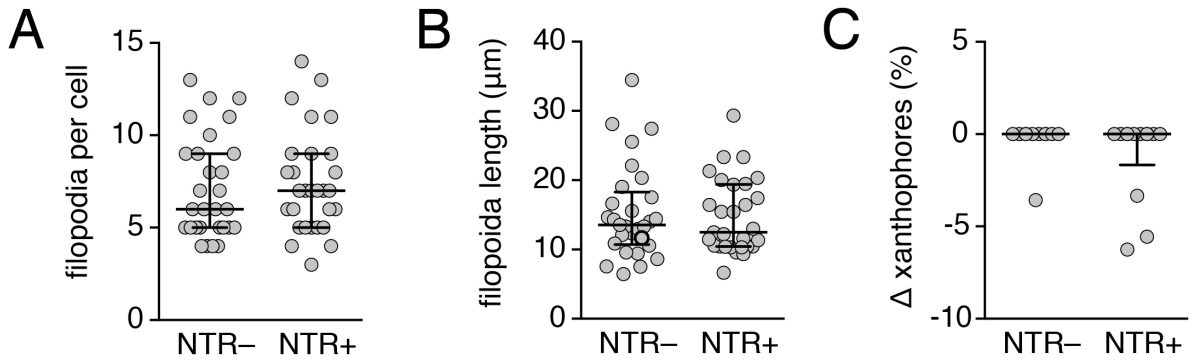

Supplementary figure S5. Mtz treatment did not affect airineme-independent xanthoblast behaviors. *aox5*+ xanthoblasts cells in Mtz-treated larvae without *mpeg1:NTR-eYFP* (NTR–) or with *mpeg1:NTR-eYFP* (NTR+) did not differ in the numbers of typical filopodia [straight, lacking vesicles (9)] produced per cell (A; $F_{1,56}$=0.1, P=0.7), length of these filopodia (B; $F_{1,56}$=0.1, P=0.7), or persistence through time-lapse imaging (C; $F_{1,22}$=1.2, P=0.3). An increase in the number of melanophores during imaging of Mtz-treated larvae also did not differ depending on NTR transgene absence or presence (means±SE=28±3%, 21±2%; $F_{1,29}$=3.0, P=0.09).

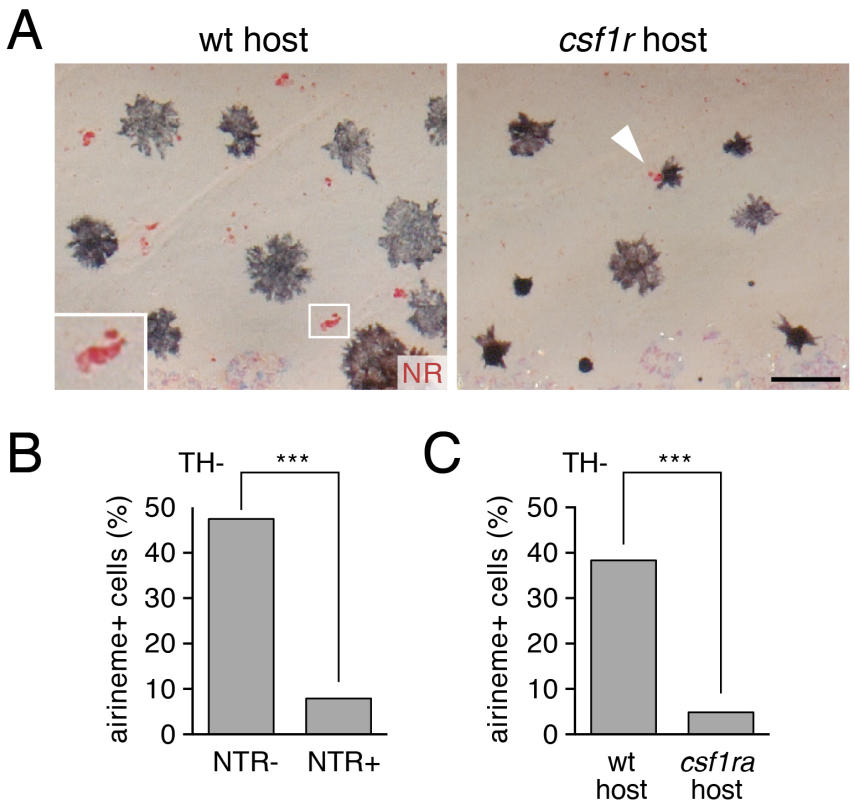

Supplementary figure S6. Macrophage depletion in chimeric larvae and airineme dependence on macrophages in hypothyroid fish. (**A**) Macrophages phagocytosing neutral red (NR) were abundant in wild-type hosts into which wild-type xanthoblasts had been transplanted (boxed region, inset) but very few macrophages (arrowhead, right) were evident in *csf1r* hosts selected to have transplanted wild-type xanthoblasts. (**B**, **C**) In *Tg(tg:nVenus-2a-NTR)* fish lacking thyroid hormone (TH-) owing to transgenic ablation of the thyroid gland, xanthophore differentiation is arrested resulting in an increased proportion of xanthoblasts competent to extend airinemes and more exuberant airineme production (6, 9). Even in TH- fish, reduced incidences of airineme extension were observed upon macrophage depletion with NTR (χ^2=16.5, d.f.=1, P<0.0001, N=78 cells, 9 larvae) or transplantation of wild-type cells to *csf1ra* mutant hosts (χ^2=49.5, d.f.=1, P<0.0001, N=292 cells, 10 larvae). Scale bar: 50 μm (A).

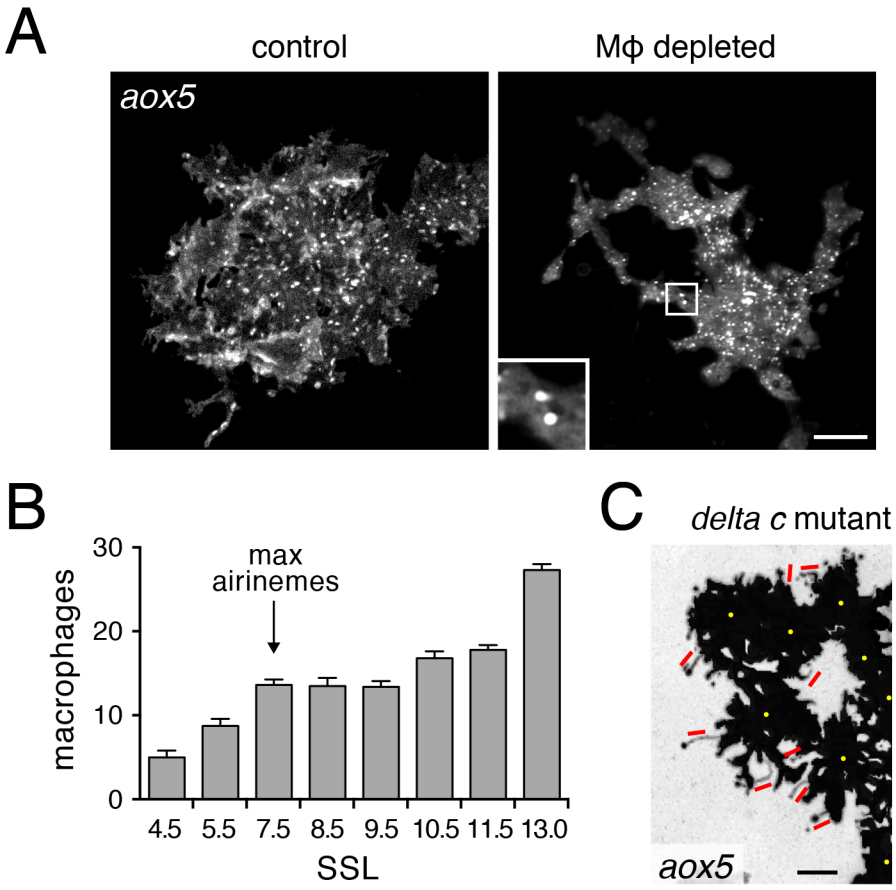

Supplementary figure S7. Macrophage-independence of xanthoblast airineme-initiating blebs and extension of airinemes in the absence of Delta C. (**A**) Surface blebs were evident in individual *aox5*$^{+}$ xanthoblasts both in macrophage-intact and macrophage depleted (*mpeg:NTR*+) fish (inset, higher magnification of two blebs in boxed region). (**B**) Despite peak airineme production at 7.5 SSL (9) *mpeg1*$^{+}$ macrophage densities (cells per 200 µm^2) increased gradually from early larva (4.5 SSL) to juvenile (13.0 SSL) (5) (*N*=41 larvae total; plots shows means±SE). (**C**) Time-lapse frames merged over 165 min illustrate normal extension of airinemes (red bars) in *delta c* mutants. Yellow dots indicate approximate positions of cell centroids. Scale bars: 10 µm (A); 25 µm (C).

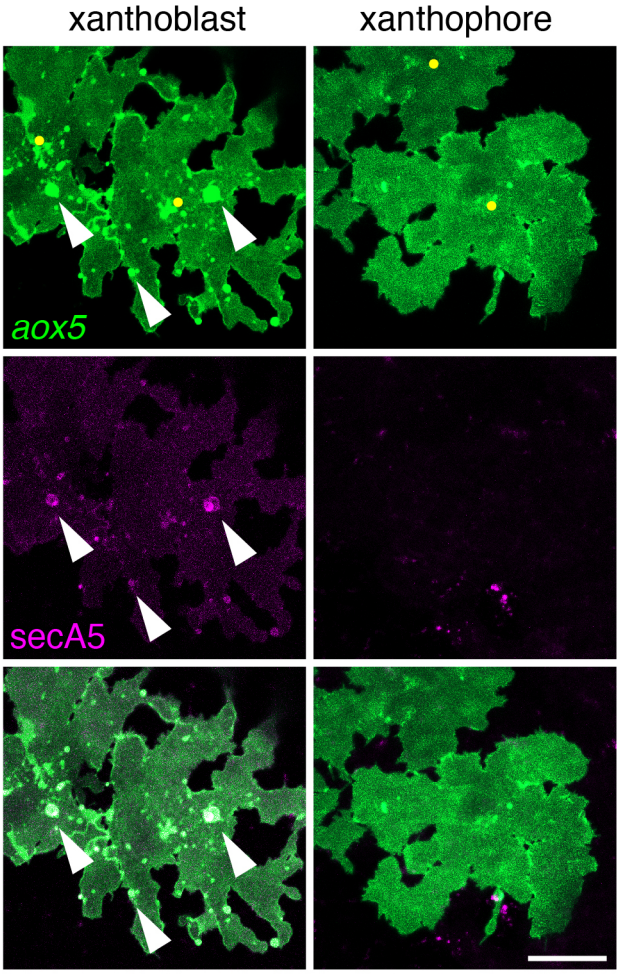

Supplementary figure S8. secA5-mCherry labeling of xanthoblasts but not xanthophores. secA5 labels blebs of xanthoblasts (left; e.g., arrowheads) but neither blebs nor secA5 labeling is observed in pigmented xanthophores (right; fluorescent puncta are secA5 expression by nearby iridophores). Yellow dots in upper panels indicate approximate positions of cell centroids. Scale bar, 50 μm.

Movie S1. Macrophage-associated airineme extension 1. Airineme (arrow) of *aox5*+ xanthoblast (green) extends in concert with migration by a passing *mpeg1*+ macrophage (blue). Minutes elapsed at upper left.

Movie S2. Macrophage-associated airineme extension 2. An airineme vesicle (arrow) and long trailing filament extend in association with a wandering macrophage (arrowhead). Minutes elapsed at upper left.

Movie S3. Macrophage-associated airineme extension 3. An airineme extended slowly (arrow) in association with a slow-moving macrophage. Hours and minutes elapsed at upper left.

Movie S4. Macrophage-associated airineme extension 4. Several airinemes (arrowheads) extended with migrating macrophages in an time-lapse imaged intact larva, similar to *ex vivo* imaging (see Materials and methods). Partial retraction following macrophage-vesicle dissociation suggests membrane tension. Hours and minutes elapsed at upper left.

Movie S5. Airineme extension associated with more than one macrophage. A wandering macrophage (white arrowhead) passed a xanthoblast and associated with an airineme vesicle (arrow). After the airineme detached from the first macrophage, a second pass macrophage (yellow arrowhead) associated with the remaining vesicle and filament and airineme extension continued. Minutes elapsed at upper left.

Movie S6. Macrophage associations with xanthoblast and airineme. High resolution still image showing *mfap4*+ macrophages (blue) associated with *aox5*+ xanthoblast cell body (green) and airineme with either or both cells surface-rendered.

Movie S7. Macrophage ablation reveals requirement for airineme extension. Left, In non-transgenic control sibling treated with Mtz, airinemes were extended frequently (arrows); macrophages are not visible owing to absence of the transgene. In an *mpeg1:NTR-eYFP*+ sibling treated with Mtz to ablate macrophages, no airinemes were observed. Blue *mpeg1*+ puncta are macrophage debris. Hours and minutes elapsed at upper left.

Movie S8. Airinemes are not extended in macrophage deficient mutants. Left, Wild-type xanthoblasts transplanted to wild-type hosts frequently extended airinemes (arrows). Wild-type xanthoblasts transplanted to macrophage-deficient *csf1ra* mutant hosts failed to extend airinemes. Hours and minutes elapsed at upper left.

Movie S9. Macrophage ablation prevents airineme extension in fish arrested for xanthophore differentiation. In fish lacking thyroid hormone (TH-), xanthophore differentiation is inhibited such that *aox5*+ cells are arrested at an airineme-producing xanthoblast state (9). Despite the enhanced competence of *aox5*+ cells to produce airinemes, NTR-mediated macrophage ablation resulted in a failure of airineme extension. Left, control individual (NTR+ Mtz-) showing airinemes (arrows) and macrophages (blue). Right, macrophage-depleted individual (NTR+ Mtz+) showing lack or airinemes and macrophage debris. Hours and minutes elapsed at upper left.

Movie S10. Lack of airineme extension in macrophage-deficient fish arrested for xanthophore differentiation. In TH-, macrophage-deficient *csf1ra* mutants, transplanted wild-type xanthoblasts failed to extend airinemes. Left, wild-type xanthoblasts transplanted to TH-, wild-type hosts extended airinemes frequently (arrows). Right, wild-type xanthoblasts transplanted to TH-, macrophage-deficient *csf1ra* hosts failed to extend airinemes. Hours and minutes elapsed at upper left.

Movie S11. Rare airinemes in macrophage-depleted fish were associated with residual macrophages. Example of airineme (arrow) extending with a macrophage (arrowhead) that persisted after Mtz treatment in an individual transgenic for *mpeg1:NTR-eYFP*. Hours and minutes elapsed at upper left.

Movie S12. Macrophage-mediated airineme delivery to melanophore. A macrophage (blue, arrowhead) migrates ventrally with associated airineme (green, arrow), the vesicle and filament of which stabilize on a melanophore (magenta) as the macrophage continues to migrate with vesicular material. Left, *mpeg1*$^{+}$ macrophages and *aox5*$^{+}$ xanthoblasts and airinemes. Right, three color merge showing *tyrp1b*$^{+}$ melanophores as well. Hours and minutes elapsed at upper left.

Movie S13. Macrophage-mediated airineme delivery to melanophore. Extension of macrophage associated airineme and stabilization on melanophore (see movie S12 legend).

Movie S14. Macrophage clearance of airineme vesicle. As an airineme filament and vesicle (greenish white) stabilized initially on a melanophore (magenta) degenerated, vesicle and other debris were cleared by successive, passing macrophages (arrowheads). Hours and minutes elapsed at upper left.

Movie S15. Macrophage clearance of airineme vesicle. Debris from airineme vesicle and filament (arrow) were cleared by macrophages (arrowheads). Circles indicate autofluorescent puncta of xanthophore pigment associated with cells not carrying the *aox5* transgene.

Movie S16. Macrophage clearance of unstabilized airineme vesicle. A macrophage (arrowhead) initially associated with an extending airineme vesicle (arrow) continued to migrate when airineme filament is severed, after which vesicle-associated fluorescence is lost, presumably owing to complete phagocytosis and digestion.

References

1. A. I. Tauber, Metchnikoff and the phagocytosis theory. *Nat. Rev. Mol. Cell Biol.* **4**, 897–901 (2003). doi:10.1038/nrm1244 Medline

2. J. A. Stefater 3rd, S. Ren, R. A. Lang, J. S. Duffield, Metchnikoff's policemen: Macrophages in development, homeostasis and regeneration. *Trends Mol. Med.* **17**, 743–752 (2011). doi:10.1016/j.molmed.2011.07.009 Medline

3. T. A. Wynn, A. Chawla, J. W. Pollard, Macrophage biology in development, homeostasis and disease. *Nature* **496**, 445–455 (2013). doi:10.1038/nature12034 Medline

4. F. Ginhoux, S. Jung, Monocytes and macrophages: Developmental pathways and tissue homeostasis. *Nat. Rev. Immunol.* **14**, 392–404 (2014). doi:10.1038/nri3671 Medline

5. D. M. Parichy, M. R. Elizondo, M. G. Mills, T. N. Gordon, R. E. Engeszer, Normal table of postembryonic zebrafish development: Staging by externally visible anatomy of the living fish. *Dev. Dyn.* **238**, 2975–3015 (2009). doi:10.1002/dvdy.22113 Medline

6. S. K. McMenamin, E. J. Bain, A. E. McCann, L. B. Patterson, D. S. Eom, Z. P. Waller, J. C. Hamill, J. A. Kuhlman, J. S. Eisen, D. M. Parichy, Thyroid hormone-dependent adult pigment cell lineage and pattern in zebrafish. *Science* **345**, 1358–1361 (2014). doi:10.1126/science.1256251 Medline

7. S. Curado, D. Y. Stainier, R. M. Anderson, Nitroreductase-mediated cell/tissue ablation in zebrafish: A spatially and temporally controlled ablation method with applications in developmental and regeneration studies. *Nat. Protoc.* **3**, 948–954 (2008). doi:10.1038/nprot.2008.58 Medline

8. T. A. Petrie, N. S. Strand, C. T. Yang, J. S. Rabinowitz, R. T. Moon, Macrophages modulate adult zebrafish tail fin regeneration. *Development* **141**, 2581–2591 (2014). doi:10.1242/dev.098459 Medline

9. D. S. Eom, E. J. Bain, L. B. Patterson, M. E. Grout, D. M. Parichy, Long-distance communication by specialized cellular projections during pigment pattern development and evolution. *eLife* **4**, e12401 (2015). doi:10.7554/eLife.12401 Medline

10. E. H. Budi, L. B. Patterson, D. M. Parichy, Post-embryonic nerve-associated precursors to adult pigment cells: Genetic requirements and dynamics of morphogenesis and differentiation. *PLOS Genet.* **7**, e1002044 (2011). doi:10.1371/journal.pgen.1002044 Medline

11. D. M. Parichy, J. M. Turner, Temporal and cellular requirements for Fms signaling during zebrafish adult pigment pattern development. *Development* **130**, 817–833 (2003). doi:10.1242/dev.00307 Medline

12. H. Hamada, M. Watanabe, H. E. Lau, T. Nishida, T. Hasegawa, D. M. Parichy, S. Kondo, Involvement of Delta/Notch signaling in zebrafish adult pigment stripe patterning. *Development* **141**, 318–324 (2014). doi:10.1242/dev.099804 Medline

13. M. Watanabe, S. Kondo, Is pigment patterning in fish skin determined by the Turing mechanism? *Trends Genet.* **31**, 88–96 (2015). doi:10.1016/j.tig.2014.11.005 Medline

14. U. Irion, A. P. Singh, C. Nüsslein-Volhard, The developmental genetics of vertebrate color pattern formation: Lessons from zebrafish. *Curr. Top. Dev. Biol.* **117**, 141–169 (2016). doi:10.1016/bs.ctdb.2015.12.012 Medline

15. A. Nakamasu, G. Takahashi, A. Kanbe, S. Kondo, Interactions between zebrafish pigment cells responsible for the generation of Turing patterns. *Proc. Natl. Acad. Sci. U.S.A.* **106**, 8429–8434 (2009). doi:10.1073/pnas.0808622106 Medline

16. M. Inaba, H. Yamanaka, S. Kondo, Pigment pattern formation by contact-dependent depolarization. *Science* **335**, 677 (2012). doi:10.1126/science.1212821 Medline

17. E. M. Walton, M. R. Cronan, R. W. Beerman, D. M. Tobin, The macrophage-specific promoter mfap4 allows live, long-term analysis of macrophage behavior during mycobacterial infection in zebrafish. *PLOS ONE* **10**, e0138949 (2015). doi:10.1371/journal.pone.0138949 Medline

18. J. Dai, M. P. Sheetz, Membrane tether formation from blebbing cells. *Biophys. J.* **77**, 3363–3370 (1999). doi:10.1016/S0006-3495(99)77168-7 Medline

19. D. M. Parichy, D. G. Ransom, B. Paw, L. I. Zon, S. L. Johnson, An orthologue of the kit-related gene fms is required for development of neural crest-derived xanthophores and a subpopulation of adult melanocytes in the zebrafish, *Danio rerio*. *Development* **127**, 3031–3044 (2000). Medline

20. P. Herbomel, B. Thisse, C. Thisse, Zebrafish early macrophages colonize cephalic mesenchyme and developing brain, retina, and epidermis through a M-CSF receptor-dependent invasive process. *Dev. Biol.* **238**, 274–288 (2001). doi:10.1006/dbio.2001.0393 Medline

21. J. Savill, I. Dransfield, C. Gregory, C. Haslett, A blast from the past: Clearance of apoptotic cells regulates immune responses. *Nat. Rev. Immunol.* **2**, 965–975 (2002). doi:10.1038/nri957 Medline

22. A. Hochreiter-Hufford, K. S. Ravichandran, Clearing the dead: Apoptotic cell sensing, recognition, engulfment, and digestion. *Cold Spring Harb. Perspect. Biol.* **5**, a008748 (2013). doi:10.1101/cshperspect.a008748 Medline

23. S. Krahling, M. K. Callahan, P. Williamson, R. A. Schlegel, Exposure of phosphatidylserine is a general feature in the phagocytosis of apoptotic lymphocytes by macrophages. *Cell Death Differ.* **6**, 183–189 (1999). doi:10.1038/sj.cdd.4400473 Medline

24. T. J. van Ham, J. Mapes, D. Kokel, R. T. Peterson, Live imaging of apoptotic cells in zebrafish. *FASEB J.* **24**, 4336–4342 (2010). doi:10.1096/fj.10-161018 Medline

25. L. B. Patterson, D. M. Parichy, Interactions with iridophores and the tissue environment required for patterning melanophores and xanthophores during zebrafish adult pigment stripe formation. *PLOS Genet.* **9**, e1003561 (2013). doi:10.1371/journal.pgen.1003561 Medline

26. C. L. Fairchild, M. Barna, Specialized filopodia: At the 'tip' of morphogen transport and vertebrate tissue patterning. *Curr. Opin. Genet. Dev.* **27**, 67–73 (2014). doi:10.1016/j.gde.2014.03.013 Medline

27. T. B. Kornberg, S. Roy, Cytonemes as specialized signaling filopodia. *Development* **141**, 729–736 (2014). doi:10.1242/dev.086223 Medline

28. M. C. McKinney, D. A. Stark, J. Teddy, P. M. Kulesa, Neural crest cell communication involves an exchange of cytoplasmic material through cellular bridges revealed by photoconversion of KikGR. *Dev. Dyn.* **240**, 1391–1401 (2011). doi:10.1002/dvdy.22612 Medline

29. M. Inaba, M. Buszczak, Y. M. Yamashita, Nanotubes mediate niche-stem-cell signalling in the *Drosophila* testis. *Nature* **523**, 329–332 (2015). doi:10.1038/nature14602 Medline

30. H. Meinhardt, A. Gierer, Pattern formation by local self-activation and lateral inhibition. *Bioessays* **22**, 753–760 (2000). doi:10.1002/1521-1878(200008)22:8<753:AID-BIES9>3.0.CO;2-Z Medline

31. A. J. Pagán, C.-T. Yang, J. Cameron, L. E. Swaim, F. Ellett, G. J. Lieschke, L. Ramakrishnan, Myeloid growth factors promote resistance to mycobacterial infection by curtailing granuloma necrosis through macrophage replenishment. *Cell Host Microbe* **18**, 15–26 (2015). doi:10.1016/j.chom.2015.06.008 Medline

32. K. M. Kwan, E. Fujimoto, C. Grabher, B. D. Mangum, M. E. Hardy, D. S. Campbell, J. M. Parant, H. J. Yost, J. P. Kanki, C.-B. Chien, The Tol2kit: A multisite gateway-based construction kit for Tol2 transposon transgenesis constructs. *Dev. Dyn.* **236**, 3088–3099 (2007). doi:10.1002/dvdy.21343 Medline

33. D. S. Eom, S. Inoue, L. B. Patterson, T. N. Gordon, R. Slingwine, S. Kondo, M. Watanabe, D. M. Parichy, Melanophore migration and survival during zebrafish adult pigment stripe development require the immunoglobulin superfamily adhesion molecule Igsf11. *PLOS Genet.* **8**, e1002899 (2012). doi:10.1371/journal.pgen.1002899 Medline